Microelectronics Reliability 88–90 (2018) 1189–1194

Contents lists available at ScienceDirect

Microelectronics Reliability

journal homepage: www.elsevier.com/locate/microrel

Remaining useful life prediction for lithium-ion batteries based on an integrated health indicator

Yongquan Sun[a,b,*], Xueling Hao[a], Michael Pecht[b], Yapeng Zhou[c,b]

[a] ISRE, Harbin University of Science and Technology, Harbin, China
[b] CALCE, University of Maryland, College Park, MD 20742, USA
[c] Wuhan University of Technology, Wuhan 430070, China

ARTICLE INFO

Keywords:
Lithium-ion battery
Remaining useful life
State of health
Integrated health indicator
Particle filter

ABSTRACT

State of health estimation and remaining useful life prediction of lithium-ion batteries is challenging due to various health indicators characterizing battery degradation. This paper develops an integrated health indicator to predict remaining useful life by incorporating capacitance, resistance, and constant current charge time with the help of a beta distribution function, based on the correlation analysis between parameter variations and aging mechanisms. A three-order polynomial model is employed to fit the battery health degradation process, remaining useful life is predicted using a particle filter algorithm, and the probability density function for the battery remaining useful life is then provided. A case study is conducted to validate the health degradation model and battery remaining useful life prediction. The results show that the constant voltage charge time is not a good health indicator, and a threshold of 0.85 is recommended as the end-of-life criterion based on the integrated health indicator. The developed method provides a reference for battery remaining useful life prediction when sufficient energy and power are required.

1. Introduction

Lithium-ion batteries are regarded as the most promising energy candidate in the automotive industry [1]. Since battery performance inevitably degrades with cycling, information about the state of health (SOH) of lithium-ion batteries is critical for safe and reliable operation [2]. Generally, the remaining useful life (RUL) is predicted to give users an estimate of battery cycle life, so that decisions on battery replacement can be made. However, controversies exist for how the SOH indicators are determined. This paper develops a new integrated health indicator, from the point of view of capacitance and power, to represent battery SOH and predict battery RUL.

Generally, capacity and internal resistance are employed to represent battery SOH [3]. For example, a capacity lower than 80% is considered as the criterion for end-of-life (EOL) [4], and electrochemical impedance spectroscopy is used to measure a battery's internal resistance and characterize the varying aging and fault processes [5]. Because batteries in plug-in hybrid vehicles (PHEVs) require sufficient energy and power [6], and power fades when resistance increases as the battery ages [7], both the capacity and internal resistance should be integrated to estimate battery SOH. In addition, Eddahech et al. [8] explored an SOH determination method based on constant voltage charge time (CVCT). Williard et al. [9] introduced the beta distribution function to combine capacitance, resistance, constant current charge time (CCCT), and CVCT to produce a new SOH indicator. However, they did not validate the effectiveness through aging mechanism analysis on the CCCT or CVCT. Nor did they focus on RUL prediction based on the fused indicator or a single indicator. Therefore, this paper correlates the parameter variations of CCCT and CVCT to the aging mechanisms and develops a new integrated SOH indicator.

Estimating battery SOH and predicting RUL is difficult because batteries are sophisticated nonlinear systems with elusive chemical reactions [10]. Thus, many data training algorithms have been applied to predict battery RUL. Terzimehic et al. [11] applied support vector machine (SVM) to predict RUL using load collectives as the training and test data. Jiang et al. [12] used genetic algorithm (GA) to estimate the battery model parameters, and then determined the battery RUL using the identified diffusion capacitance. Because the particle filter (PF) is able to provide the probability distribution, it has become one of the most effective important methods to predict RUL. The PF was used for RUL prediction based on a state-space model [13]. Dempster–Shafer (DS) theory and the PF method were combined to predict battery RUL [14]. This paper uses a three-order polynomial model and the PF algorithm to predict battery RUL based on an integrated health indicator.

* Corresponding author at: ISRE, Harbin University of Science and Technology, Harbin, China.
E-mail address: sunyongquan@sina.com (Y. Sun).

https://doi.org/10.1016/j.microrel.2018.07.047
Received 13 May 2018; Accepted 4 July 2018
Available online 30 September 2018

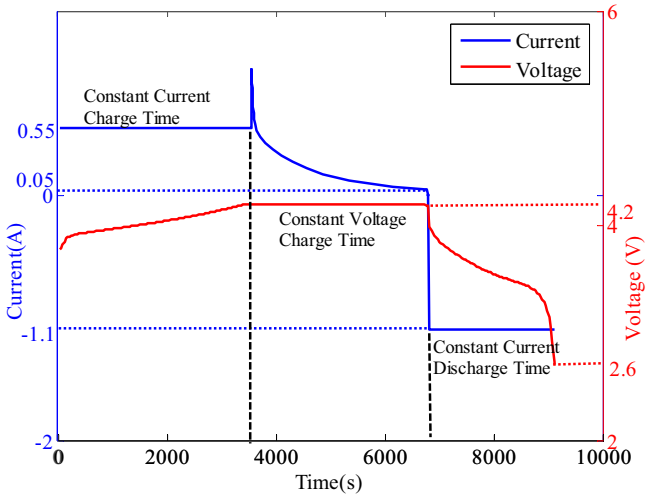

Fig. 1. Charge/discharge profile. A constant charge current of 0.55 A was applied until the voltage reached 4.2 V, and then 4.2 V was sustained until the current fell to below 0.05 A. A typical constant current discharge at 1.1 A, and the cut-off voltage was 2.7 V.

The remainder of this paper is organized as follows. Section 2 deals with the identification of the integrated SOH indicator. Section 3 describes the RUL prediction method in detail. Section 4 validates the model and discusses the prediction results. Section 5 presents the conclusions.

2. Identification of the integrated SOH indicator

Three battery cells with a rated capacity of 1.1 Ah underwent cycle life tests using Arbin BT2000 test equipment under room temperature. The testing profile is shown in Fig. 1. Capacitance, resistance, CCCT, and CVCT were measured as shown in Fig. 2. The capacitance and CCCT decreased with cycles, whereas the resistance and CVCT increased with cycles. The peak point observed in Fig. 2d could indicate specific internal degradation mechanisms that are not as apparent in the discharge capacity in (a) and the CCCT in (c).

When the constant current charge process begins, the applied current forces the lithium ions to move from the anode to the cathode, leading to a negative concentration gradient inside the cathode, separators, and anode [15]. The concentration gradient increases progressively along the current flow trail and reaches the maximum at the end of the constant current charge stage.

Because of solid electrolyte interface (SEI) layer growth, the internal resistance continues to increase with aging and reduces the CCCT due to continuous increase of the voltage drop on the SEI layer. Moreover, the available charge quantity of the cathode material decreases with aging, which also contributes to the cell voltage reaching the cutoff value earlier, resulting in a decrease in total charging time with aging [16]. A correlation analysis between CCCT and capacitance and resistance is presented in Fig. 3. Therefore, the EOL for a battery can be determined to be the time when the battery capacity is 80% lower than the initial value.

Throughout the constant voltage charge stage, the current drops rapidly, leading the lithium ion concentration gradient to decrease from the maximum to a minimal level as the constant voltage step reaches the end when the current falls to below 0.05 A. Eddahech et al. [8] considered the constant voltage step is responsible for most of the lithium intercalation into the negative electrode, and applied the constant voltage step as the SOH indicator.

As shown in Fig. 4, when the CVCT is measured, it is difficult to

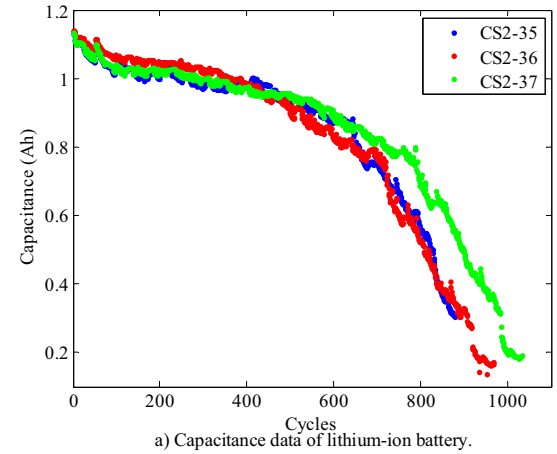

a) Capacitance data of lithium-ion battery.

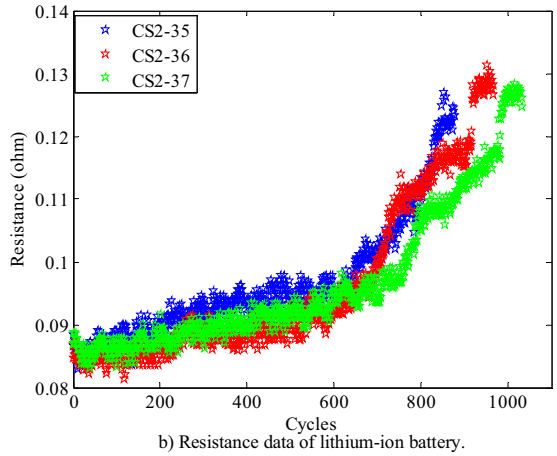

b) Resistance data of lithium-ion battery.

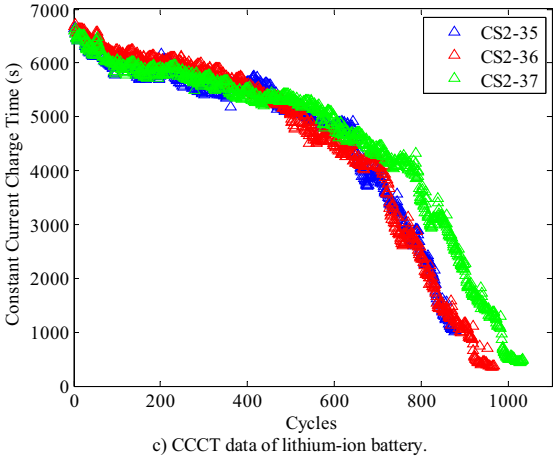

c) CCCT data of lithium-ion battery.

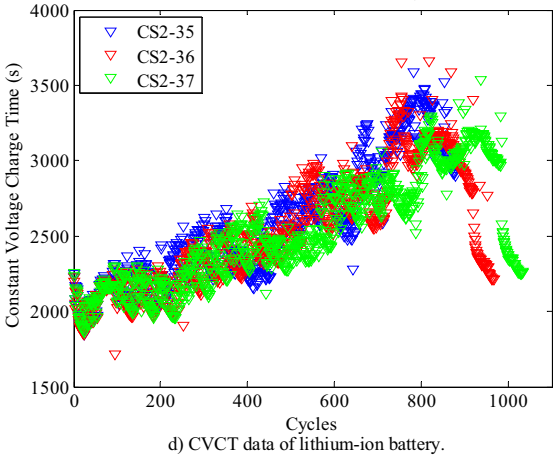

d) CVCT data of lithium-ion battery.

(caption on next page)

Fig. 2. Experiment data for cells CS2-35/CS2-36/CS2-37.

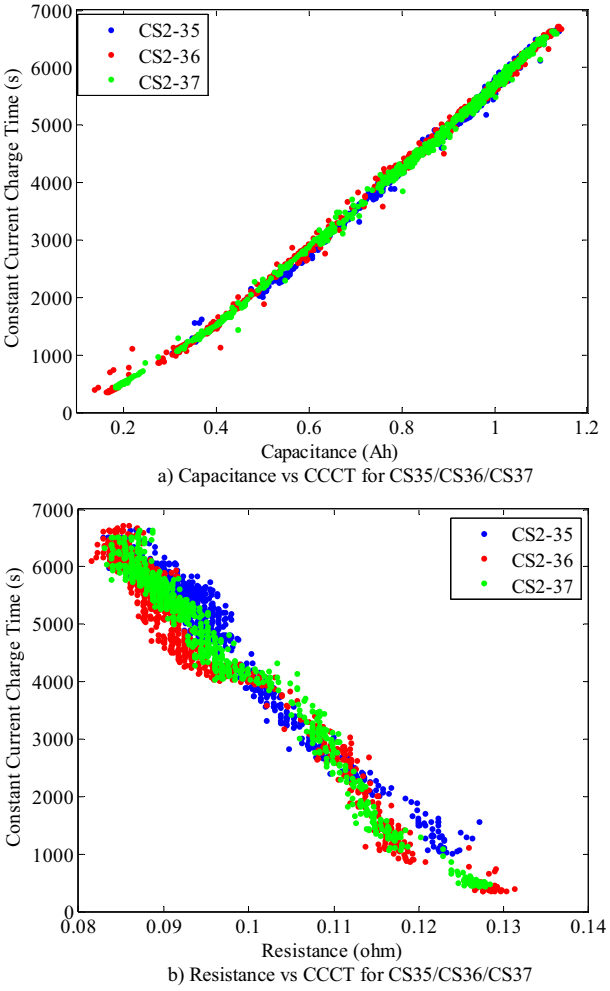

Fig. 3. Incidence relationship between CCCT and capacitance and resistance. The CCCT has a linear relationship with the capacitance as shown in (a).

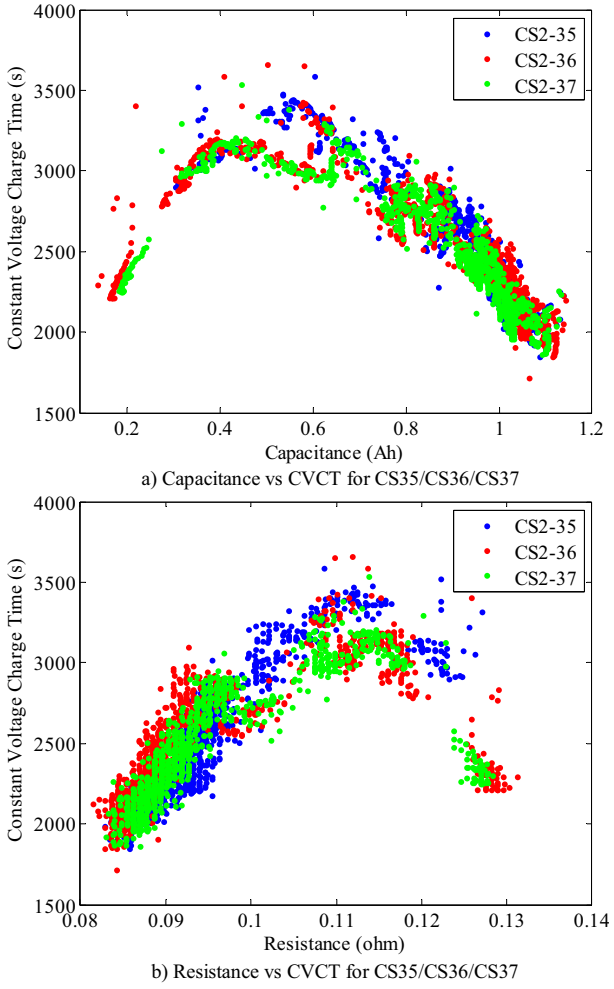

Fig. 4. Incidence relationship between CVCT and capacitance and resistance. Both the curves in (a) and (b) are non-monotonic, and include one peak point.

identify the specific value of the capacitance or resistance. Therefore, the CVCT is not a good indicator of battery SOH. According to Peled and Menkin [17], the SEI layers are divided into a compact layer and a secondary layer. The secondary SEI forms a more porous or structurally open layer than the compact layer and suppresses the mass transport of ions in the electrolyte, filling its pores. This SEI layer suffers from much more lithium exhaustion [18]. It can be concluded that the CVCT is derived from both the decreasing capacitance and increasing internal resistance, but the latter contributes more to the rise of CVCT at the early aging period, and the former contributes more to the reduction of CVCT at the later aging period. Therefore, the capacitance, resistance, and CCCT should be incorporated into battery SOH estimation and RUL prediction, whereas the CVCT is not a good SOH indicator.

A normalization transition was carried out as follows: $Cap_N(k) = Cap(k) / \text{Ini\_Cap}$, $CCCT_N(k) = CCCT(k) / \text{Ini\_CCCT}$, $Res_N(k) = (R_{EOL} - Res(k)) / \text{Ini\_Res}$, where $Cap_N(k)$, $CCCT_N(k)$, and $Res_N(k)$ are the normalized indicators for capacitance $Cap(k)$, $CCCT(k)$, and resistance $Res(k)$, and Ini_Cap, Ini_Res, and Ini_CCCT are the initial values respectively; k is the cycle number; and $R_{EOL} = 2$ Ini_Res is the internal resistance at the EOL.

The integrated SOH indicator was computed with the help of the beta distribution function $f_k(SOH_k; \alpha_k, \beta_k)$, where α_k and β_k are distribution parameters and SOH_k is estimated by

$$SOH_k = \alpha_k/(\alpha_k + \beta_k) = \sum_{j=1}^{3} w_{j,k} d_{j,k} / \sum_{j=1}^{3} w_{j,k} \quad (1)$$

where $d_{j,k}$ ($j = 1, 2, 3$) are observations of indicators at cycle k, for $j = 1$ is capacitance, $j = 2$ is resistance, and $j = 3$ is CCCT, $w_{j,k}$ is the weight of the indicator $d_{j,k}$, and the initial weights $w_{j,1} = 1/3$ when $k = 1$.

When the observations of the indicators of the next cycle $k + 1$ are obtained, then the weights are updated based on the following equation,

$$w_{j,k+1} = w_{j,k} + (1 - | SOH_k - d_{j,k} |) \quad (2)$$

3. RUL prediction based on PF algorithm

A three-order polynomial model was employed to fit the battery degradation process with a trade-off between model accuracy and calculation complexity,

$$S = a_1 \times k^3 + a_2 \times k^2 + a_3 \times k + a_4 \quad (3)$$

where S is the health state of the battery; and a_1, a_2, a_3, a_4 are model parameters. The parameter estimates can be computed with the help of Matlab. The state transfer equation of a lithium-ion battery is

$$x_k = [a_{1,k}\ a_{2,k}\ a_{3,k}\ a_{4,k}]^T \rightarrow p(x_k/x_{k-1}) \quad (4)$$

where $a_{r,k} = a_{r,k-1} + v_{ar}(k)$, $v_{ar}(k) \sim N(0,\delta_v)$ are Gaussian noise with zero mean and standard deviation δ_v; $p(x_k/x_{k-1})$ is the transition distribution; and r (r = 1, 2, 3, 4) stands for the order of parameters. The initial state value is $x_0 = [a_{1,0},\ a_{2,0},\ a_{3,0},\ a_{4,0}]^T$. The measurement equation is

$$S_k = a_{1,k}k^3 + a_{2,k}k^2 + a_{3,k}k + a_{4,k} + \mu(k), \rightarrow p(S_k/x_k) \tag{5}$$

where $\mu(k)$ is the measurement of Gaussian white noise with zero mean and standard deviation δ_μ, $\mu(k) \sim N(0,\delta_\mu)$, and $p(S_k/x_k)$ is the observation distribution.

Given the PDF of the initial state $p(x_0/S_0) = p(x_0)$, when the measurement S_k of status x_k is observed, the PDF is denoted as $p(S_k/x_k)$, then the posterior PDF of status x_k is updated [13],

$$p(x_k/S_k) = p(S_k/x_k)\, p(x_k/S_{k-1})/p(S_k/S_{k-1}) \tag{6}$$

where the constant $p(S_k/S_{k-1}) = \int p(S_k/x_k)\ p(x_k/S_{k-1})\mathrm{d}x_k$, $p(x_k/S_{k-1}) = \int p(x_k/x_{k-1})p(x_{k-1}/S_{k-1})\ \mathrm{d}x_{k-1}$.

The particle filter is applied to approximate the posterior PDF using a set of particles x_k^i (i = 1, …, N) with the associated weights w_k^i. The particles x_k^i and weight $w_k^i$are propagated for the kth cycle using

$$x_k^i = q(x_k^i \mid x_{k-1}^i, S_0) = p(x_k^i \mid x_{k-1}^i) \tag{7}$$

$$w_k^i = w_{k-1}^i p(S_k/x_k^i) p(x_k^i \mid x_{k-1}^i)/q(x_k^i \mid x_{k-1}^i, S_k) \tag{8}$$

With the simulation and resampling, the PDF of $x_k$can be approximated [14],

$$p(x_k/S_k) \approx \sum_{i=1}^{N} [\overline{w}_k^i \delta(x_k - x_k^i)] \tag{9}$$

In this case, x_k represents a battery SOH indicator, and the RUL is the remaining time before the battery indicator hits the pre-defined performance threshold. The posterior distribution of x_{k+l} is

$$p(x_{k+l}/S_k) \approx \sum_{i=1}^{N} [\overline{w}_k^i \delta(x_{k+l} - x_{k+l}^i)] \tag{10}$$

For each cycle where $k + l$ projects l steps ahead of the current cycle k, the estimate $p(RUL_k \geq l|x_k)$ is equal to $p(x_{k+l} \geq 0.8)$ for the integrated SOH indicator. So the posterior PDF and expectation of RUL at cycle k can be estimated by

$$p(RUL_k/S_k) \approx \sum_{i=1}^{N} [\overline{w}_k^i \delta(RUL_k - RUL_k^i)] \tag{11}$$

$$RUL_k = \sum_{i=1}^{N} \overline{w}_k^i RUL_k^i \tag{12}$$

4. Case study

The degradation model is assessed by goodness-of-fit. The parameters of the degradation model are estimated using the fused testing data of cells CS2-35, CS2-36, and CS2-37, as shown in Table 1. The fitted curves are presented in Fig. 5. The goodness-of-fit for the degradation model is estimated and shown in Table 2. The results represent the effectiveness of the degradation model, and the model can be employed to predict battery RUL.

RUL prediction results at cycle 370 for cell CS2-35 based on the integrated SOH with EOL thresholds 0.8 and 0.85 are shown in Fig. 6. The prediction results at the 370th cycle for CS2-35, including the predictor, prediction error, and standard deviation (STD), based on the capacitance, resistance, and CCCT are represented in Table 3.

The predicted RUL with an EOL threshold 0.85 is reasonable because the value is close to the predicted RUL using capacitance, and this threshold is recommended as the EOL criterion. Further investigation on the EOL criterion should be conducted based on more practical applications.

The RUL prediction results at the 400th and 500th cycle are presented in Fig. 7. The more data that were collected, the more accurate the prediction results were.

Table 1
Model parameters.

Cell no.	a_1	a_2	a_3	a_4
CS2-35	-2.73×10^{-9}	2.54×10^{-6}	−0.000897	1.0080
CS2-36	-1.40×10^{-9}	8.72×10^{-7}	−0.000387	0.9958
CS2-37	-1.61×10^{-9}	1.52×10^{-6}	−0.000628	0.9974

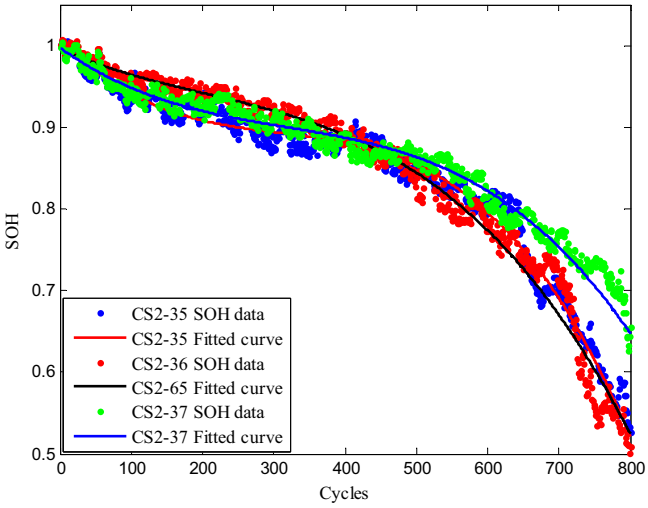

Fig. 5. SOH degradation data and fitted curves.

Table 2
Goodness-of-fit.

Cell no.	SSE	R-square	RMSE	Adjusted R-square
CS2-35	0.0237	0.9989	0.005207	0.9989
CS2-36	0.03251	0.9993	0.005807	0.9993
CS2-37	0.02035	0.9995	0.004445	0.9995

5. Conclusions

This paper developed an RUL prediction approach using an integrated SOH indicator and a particle filter algorithm. CCCT and CVCT aging mechanisms and incidence relationships with capacitance and resistance were analyzed. The CVCT is not a good SOH indicator, and the capacitance, resistance, and CCCT should be integrated to produce a new SOH indicator from the point of view of capacity and power. Consequently, a method to integrate this new SOH indicator was developed using the beta distribution function.

A modified polynomial model was employed to describe the battery SOH degradation, and the goodness-of-fit with maximum SSE = 0.03251 validated the effectiveness of the model. Moreover, an approach for RUL prediction was provided based on the integrated SOH indicator and a particle filter algorithm. The prediction results derived from the single indicator and the fused SOH indicator were compared, and a value of 0.85 was recommended as the EOL criterion based on the

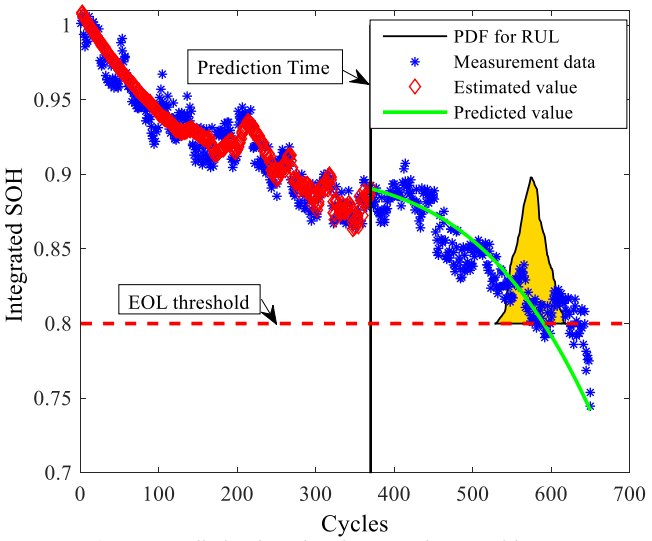

a) RUL prediction based on integrated SOH with EOL as 0.8

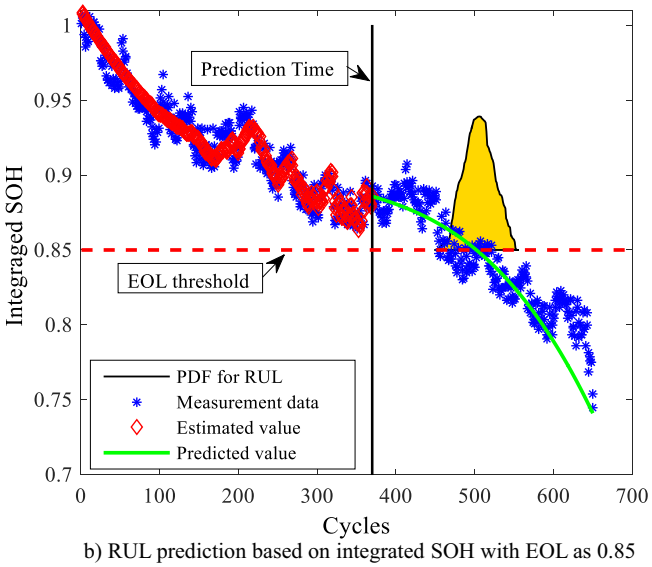

b) RUL prediction based on integrated SOH with EOL as 0.85

Fig. 6. RUL prediction at the 370th cycle for CS2-35. The maximum error of the predicted RUL from the real data is 27 cycles, and the maximum STD of the RUL is 16 cycles.

Table 3
Prediction results based on various indicators.

Indicator	Threshold	RUL (cycles)	Prediction error (cycles)	STD (cycles)
Capacitance	0.80	148	17	15
Resistance	0.00	> 430	–	–
CCCT	0.80	83	9	17
Integrated health indicator	0.80	221	21	14
	0.85	142	27	16

integrated SOH indicator. RUL predictions at the 500th cycle were found to be more accurate than those at the 400th cycle, as shown by the comparison of the prediction errors and STDs of RUL. The developed method has the potential to predict battery RUL in PHEVs when sufficient energy and power are required simultaneously.

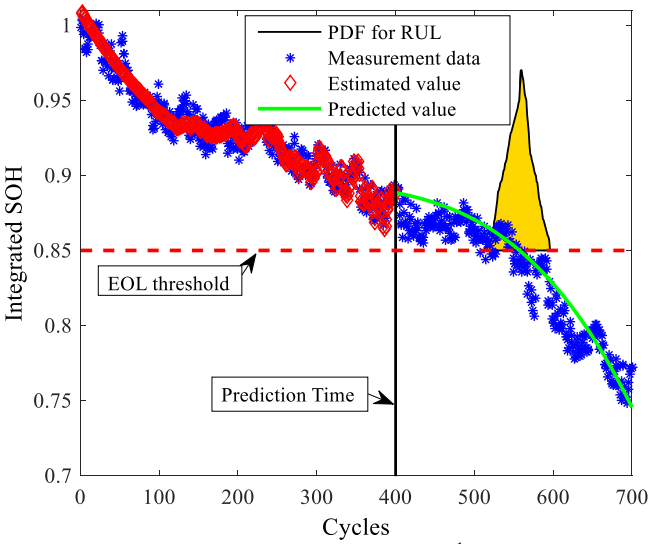

a) Prediction results at 400th cycle

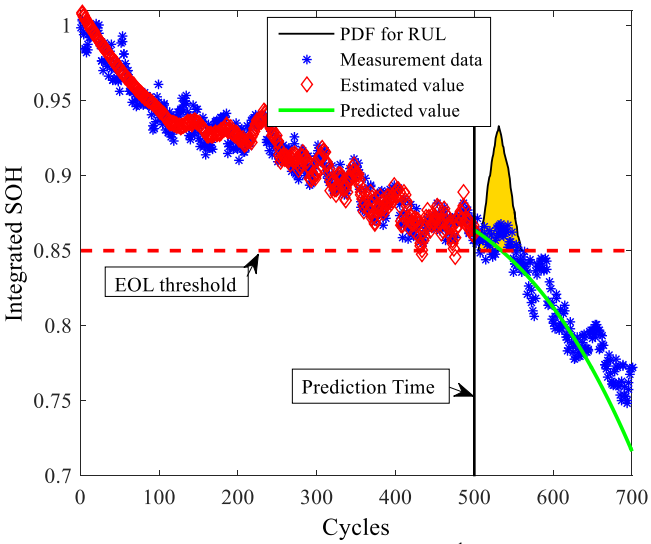

b) Prediction results at 500th cycle

Fig. 7. Prediction results at different cycles for CS2-37. The predicted RUL at the 400th cycle is around 158 cycles with a 48-cycle error, whereas, the predicted RUL at the 500th cycle is about 35 cycles with a 25-cycle error. The STD is 13 cycles and 10 cycles.

Acknowledgements

This research was sponsored by Natural Science Foundation of Heilongjiang Province (QC2016068), and University Nursing Program for Young Scholars with Creative Talents in Heilongjiang Province (UNPYSCT-2017087). The authors thank Cheryl Wurzbacher for editing and comments to improve the paper's quality.

References

[1] Z. Li, J. Huang, B.Y. Liaw, et al., On state-of-charge determination for lithium-ion batteries, J. Power Sources 348 (2017) 281–301.
[2] T.R. Ashwin, Y.M. Chung, Capacity fade modelling of lithium-ion battery under cyclic loading conditions, J. Power Sources 328 (2016) 586–598.
[3] C. Zhang, Y. He, L. Yuan, et al., Capacity prognostics of lithium-ion batteries using EMD denoising and multiple kernel RVM, IEEE Access 5 (2017) 12061–12070.

[4] Y. Zhang, R. Xiong, H. He, W. Shen, Lithium-ion battery pack state of charge and state of energy estimation algorithms using a hardware-in-the-loop validation, IEEE Trans. Power Electron. 32 (2017) 4421–4431.
[5] S. Schindler, M. Danzer, A novel mechanistic modeling framework for analysis of electrode balancing and degradation modes in commercial lithium-ion cells, J. Power Sources 343 (2017) 226–236.
[6] L. Lu, X. Han, J. Li, J. Hua, M. Ouyang, A review on the key issues for lithium-ion battery management in electric vehicles, J. Power Sources 226 (2013) 272–288.
[7] Z.G. He, D. Chen, C.F. Pan, et al., State of charge estimation of power Li-ion batteries using a hybrid estimation algorithm based on UKF, Electrochim. Acta 211 (2016) 101–109.
[8] A. Eddahech, O. Briat, J.M. Vinassa, Determination of lithium-ion battery state-of-health based on constant-voltage charge phase, J. Power Sources 258 (2014) 218–227.
[9] N. Williard, W. He, M. Osterman, M. Pecht, Comparative analysis of features for determining state of health in lithium-ion batteries, Int. J. Progn. Health Manag. 4 (2013) 1–7.
[10] R. Xiong, Y. Zhang, H. He, et al., A double-scale, particle-filtering, energy state prediction algorithm for lithium-ion batteries, IEEE Trans. Ind. Electron. 65 (2018) 1526–1538.
[11] N. Terzimehic, Health diagnosis and remaining useful life prognostics of lithium-ion batteries using data-driven methods, J. Power Sources 239 (2013) 680–688.
[12] Y.Y. Jiang, Y.R. Wang, Y. Wu, et al., Fault prognostic of electronics based on optimal multi-order particle filter, Microelectron. Reliab. 62 (2016) 167–177.
[13] Y.J. Xing, E.W.M. Ma, K.L. Tsui, M. Pecht, An ensemble model for predicting the remaining useful performance of lithium-ion batteries, Microelectron. Reliab. 53 (2013) 811–820.
[14] W. He, N. Williard, M. Osterman, M. Pecht, Prognostics of lithium-ion batteries based on Dempster–Shafer theory and the Bayesian Monte Carlo method, J. Power Sources 196 (2011) 10314–10321.
[15] S. Bashash, S.J. Moura, J.C. Forman, H.K. Fathy, Plug-in hybrid electric vehicle charge pattern optimization for energy cost and battery longevity, J. Power Sources 196 (2011) 541–549.
[16] P. Ramadass, B. Haran, P.M. Gomadam, et al., Development of first principles capacity fade model for Li-ion cells, J. Electrochem. Soc. 151 (2004) 196–203.
[17] E. Peled, S. Menkin, Review—SEI - past, present and future, J. Electrochem. Soc. 164 (2017) 1703–1719.
[18] M. Safaria, M. Morcrettea, A. Teyssotb, C. Delacourta, Multimodal physics-based aging model for life prediction of Li-ion batteries, J. Electrochem. Soc. 156 (2009) A145–A153.